Nanoscale

PAPER

View Article Online
View Journal | View Issue

Cite this: *Nanoscale*, 2017, **9**, 4550

Planar B_{38}^- and B_{37}^- clusters with a double-hexagonal vacancy: molecular motifs for borophenes†

Qiang Chen,[a,c,d] Wen-Juan Tian,[b] Lin-Yan Feng,[a] Hai-Gang Lu,[a] Yue-Wen Mu,[a] Hua-Jin Zhai,*[a] Si-Dian Li*[a] and Lai-Sheng Wang*[b]

Received 26th January 2017,
Accepted 8th March 2017

DOI: 10.1039/c7nr00641a

rsc.li/nanoscale

Boron clusters have been found to exhibit a variety of interesting electronic, structural, and bonding properties. Of particular interest are the recent discoveries of the 2D hexagonal $B_{36}^{-/0}$ which led to the concept of borophenes and the 3D fullerene-like $B_{40}^{-/0}$ which marked the onset of borospherene chemistry. Here, we present a joint photoelectron spectroscopic and first-principles study of B_{37}^- and B_{38}^-, which are in the transition size range between the 2D borophene-type clusters and the 3D borospherenes. These two clusters are found to possess highly stable 2D global-minimum structures consisting of a double-hexagonal vacancy. Detailed bonding analyses reveal that both B_{37}^- and B_{38}^- are all-boron analogues of coronene ($C_{24}H_{12}$) with a unique delocalized π system, featuring dual π aromaticity. These clusters with double hexagonal vacancies can be viewed as molecular motifs for the χ3-borophene which is the most stable form of borophenes recently synthesized on an Ag(111) substrate.

1. Introduction

Boron has a number of bulk allotropes consisting of three-dimensional (3D) cage-like structural units to compensate its electron deficiency.[1] However, early theoretical studies suggested that small boron clusters with less than 14 atoms prefer planar or quasi-planar (2D) structures.[2–8] During the past decade, the structures and bonding of size-selected boron clusters (B_n^-) have been systematically investigated using photoelectron spectroscopy (PES) and first-principles theory calculations.[9–22] This body of work has established the 2D global minima for B_n^- over a large size range up to n = 36 thus far.[23] Bonding analyses show that these 2D clusters are governed by delocalized σ and π bonding. Most interestingly, the π bonding in all 2D boron clusters can be shown to be analogous to that in polycyclic aromatic hydrocarbons (PAHs).[11,17–23,24] A joint ion mobility and density functional theory (DFT) study on cationic B_n^+ clusters with n up to 25 revealed a structural transition from 2D to tubular-type structures at n = 16,[25,26] even though tubular-type structures have not been observed for any anionic B_n^- clusters.[23]

The 2D boron clusters exhibit a wide range of structural patterns consisting of B_3 triangles and tetragonal, pentagonal, or hexagonal vacancies (holes) as "defects" in an otherwise triangular 2D lattice.[23] The defect size increases with the cluster size from tetragonal to hexagonal. The B_{26}^- cluster has been shown recently to be the smallest boron cluster with a hexagonal hole,[18c] while the global minima of $B_{36}^{-/0}$ have been shown earlier to contain a perfect hexagonal vacancy, leading to the concept of borophenes and providing the first indirect experimental evidence for the viability of monolayered borons with hexagonal vacancies.[20] The B_{35}^- cluster was subsequently found to possess a double-hexagonal vacancy (DHV) by simply removing a hexa-coordinate B atom from the B_{36}^- cluster.[21] More intriguingly, B_{35}^- was shown to be an even more flexible motif for borophenes with different arrangements of the hexagonal holes. Subsequently, borophenes were synthesized on Ag(111) substrates,[27,28] as suggested computationally.[29,30] In particular, the observed most stable χ3-borophene has a hole-density of η = 1/5, consisting of rows of adjacent hexagonal holes connected by zigzag boron double chains (BDCs).[28,31]

The discovery of the fullerene-like D_{2d} $B_{40}^{-/0}$ cages, named borospherenes,[22] in 2014 represents another landmark in

[a]*Nanocluster Laboratory, Institute of Molecular Science, Shanxi University, Taiyuan 030006, China. E-mail: hj.zhai@sxu.edu.cn, lisidian@sxu.edu.cn*
[b]*Department of Chemistry, Brown University, Providence, Rhode Island 02912, USA. E-mail: lai-sheng_wang@brown.edu*
[c]*Beijing National Laboratory for Molecular Sciences, State Key Laboratory for Structural Chemistry of Unstable and Stable Species, Institute of Chemistry, Chinese Academy of Sciences, Beijing 100190, China*
[d]*Institute of Materials Science, Xinzhou Teachers' University, Xinzhou 034000, China*
†Electronic supplementary information (ESI) available. See DOI: 10.1039/c7nr00641a

the investigation of size-selected boron clusters. The global minimum of B_{40}^- was found to be a 2D structure with a DHV, whereas the D_{2d} B_{40}^- borospherene was slightly higher in energy. However, for neutral B_{40} the D_{2d} borospherene cage consisting of twelve interwoven BDCs was overwhelmingly the global minimum. The B_{39}^- cluster was subsequently found to consist of two nearly degenerate, axially chiral C_3 and C_2 borospherene isomers which are also dominated by interwoven BDCs.[32]

An interesting question is what are the structures of B_{37}^- and B_{38}^-? These two clusters are in the transition size range between the borophene-type 2D structures and the 3D borospherenes. A previous DFT calculation suggested that neutral B_{38} possesses a borospherene cage global minimum with a low-lying 2D isomer consisting of a DHV.[33] A subsequent comment at higher levels of theory showed that the 2D and 3D structures of B_{38} are nearly degenerate with the 2D structure slightly lower in energy.[34] However, there have been no studies on the B_{38}^- anion or on $B_{37}^{-/0}$. The two missing clusters are important to understand the structural transitions and there may be a competition between 2D and 3D isomers.

We have undertaken a joint PES and quantum chemical study on the B_{37}^- and B_{38}^- clusters in the current article. The PES spectra for both clusters display relatively well-resolved spectral features. Global minimum searches revealed that both B_{37}^- and B_{38}^- consist of 2D structures with a DHV. The 3D cage isomers are significantly higher in energy and were not present experimentally. Chemical bonding analyses show that the 2D B_{38}^- and B_{37}^- are all-boron analogues of coronene ($C_{24}H_{12}$), featuring unique dual π aromaticity.

2. Methods

2.1. Experimental methods

The experiments were performed using a magnetic-bottle PES apparatus equipped with a laser vaporization cluster source, details of which can be found elsewhere.[23,35] Briefly, boron clusters were produced by focusing a laser beam on a ^{10}B-enriched disk target. The laser-induced plasma was cooled by a high pressure He carrier gas seeded with 5% Ar. The nascent clusters were entrained by the carrier gas and underwent a supersonic expansion to produce a cold cluster beam (about 200 K).[23] Negatively charged clusters were extracted perpendicularly from the collimated cluster beam and analyzed using a time-of-flight mass spectrometer. The B_{38}^- and B_{37}^- clusters of current interest were mass-selected and decelerated before being intercepted by a detachment laser beam. Photodetachment experiments were performed using the 193 nm (6.424 eV) radiation from an ArF excimer laser. Photoelectrons were collected at nearly 100% efficiency using a magnetic-bottle and analyzed in a 3.5 m long electron flight tube. The photoelectron spectra were calibrated using the known spectrum of Au^-. The energy resolution of the instrument was $\Delta E_k/E_k \approx 2.5\%$, that is, ~25 meV for 1 eV kinetic energy electrons.

2.2. Computational methods

Global-minimum searches were first performed for B_{38}^- using both the minima-hopping algorithm[36] and the TGmin code,[20,37] in combination with manual structural constructions based on the known low-lying isomers of B_{35}^-, B_{36}^-, and B_{40}^-.[20–22] On the basis of the structural information of B_{38}^-, only the minima-hopping approach was utilized to search for the global minimum of B_{37}^-. The minima-hopping searches for B_{38}^- and B_{37}^- were done using the BIGDFT electronic structure code[38] employing a systematic wavelet basis in combination with pseudopotentials and the standard local-density approximation (LDA)[39] and the Perdew–Burke–Ernzerhof (PBE) exchange–correlation functional.[40] For each cluster anion, six independent minima-hopping runs were performed, starting from six different low-lying structures. About 1700 and 2200 stationary points were probed for B_{38}^- and B_{37}^-, respectively. TGmin searches were done for B_{38}^- to check the minima-hopping results. The TGmin code was implemented in the CP2K program[41] and employed the DFT formalism with the PBE exchange–correlation functionals[40] and the Goedecker–Teter–Hutter pseudopotential[39] with the associated double-ζ valence plus polarization (DZVP) basis set.[42] With more than 1000 stationary points probed, the TGmin searches yielded the same global minimum for B_{38}^-, as the minima-hopping runs.

The low-lying isomers of B_{38}^- and B_{37}^- were then fully re-optimized at the PBE0/6-311+G* level,[43,44] which has proved to be a reliable method for boron clusters in this size regime. Vibrational frequencies were checked to ensure that the reported isomers are true minima. We calculated the vertical detachment energies (VDEs) of the B_{38}^- and B_{37}^- global minima using the time-dependent DFT method (TD-PBE0/6-311+G*).[45] The global minimum of B_{38}^- was found to be a doublet (C_s, $^2A''$) with an unpaired electron. Electron detachment from the $^2A''$ state produced two almost degenerate neutral states: a triplet B_{38} ($^3A''$) and an open-shell singlet B_{38} ($^1A''$). Thus, the first two VDEs of B_{38}^- were calculated as the energy differences between the anion ground-state ($^2A''$) and the neutral triplet $^3A''$ and the open-shell singlet $^1A''$ states at the anion ground-state geometry, respectively. Higher VDEs were obtained by adding the singlet and triplet excitation energies of the neutral to the first two VDEs. One-electron detachment from the closed-shell B_{37}^- generates doublet neutral states only, yielding fewer detachment channels.

All calculations were performed using the Gaussian 09 package.[46] Canonical molecular orbitals (CMOs) and the adaptive natural density partitioning (AdNDP) method[47] were employed to analyze the chemical bonding. Orbital visualization was done using Molekel.[48]

3. Experimental results

The photoelectron spectra of B_{38}^- and B_{37}^- at 193 nm are shown in Fig. 1, along with the simulated spectra (*vide infra*). Spectral features are labeled with letters (X, A, B, *etc.*). All

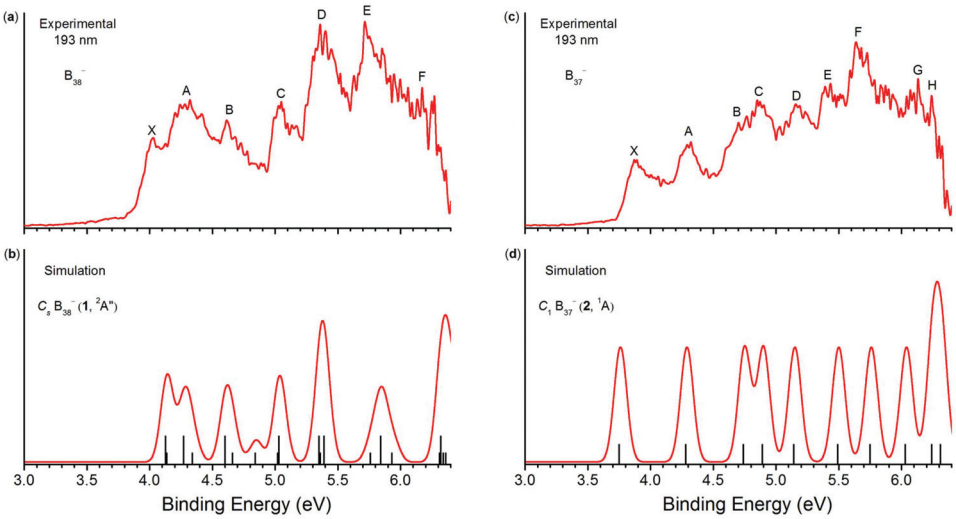

Fig. 1 Experimental photoelectron spectra of B_{38}^- (a) and B_{37}^- (c) at 193 nm (6.424 eV), compared with the simulated spectra of the global minimum C_s B_{38}^- (**1**, ^{2}A") (b) and C_1 B_{37}^- (**2**, ^{1}A) (d). The simulated spectra were recorded at the TD-PBE0/6-311+G* level by fitting the calculated VDEs (vertical bars) with unit-area Gaussian functions of 0.05 eV half-width. In (b), the longer bars are for triplet final states and the shorter bars for the singlet final states.

experimental and theoretical VDEs and adiabatic detachment energies (ADEs) are summarized in Table S1 in the ESI.†

3.1. The photoelectron spectrum of B_{38}^-

The spectrum of B_{38}^- (Fig. 1a) reveals six well-spaced bands (X, A–E), as well as continuous signals above 6 eV, labeled as F for the sake of discussion. The first VDE was evaluated from the maximum of band X to be 4.02 eV. Since no vibrational structures were resolved for this band, the ADE was estimated by drawing a straight line along its leading edge and then adding the instrumental resolution to the intersection with the binding energy axis. The ADE of B_{38}^- so obtained is 3.91 ± 0.05 eV, which also represents the electron affinity of neutral B_{38}.

Band A, centered at ~4.3 eV, is relatively broad and partially overlaps with band X. Bands B (4.62 eV) and C (5.04 eV) are sharper, followed by two intense and broader bands, D (5.39 eV) and E (5.74 eV). Neutral B_{38} has an even number of valance electrons. However, the intensity of band X is quite large relative to band A, and there exists only a small gap (~0.3 eV) between them. The ADE of B_{38}^- is also unusually large, and breaks the even–odd alternation as a function of size.[23] All these observations suggest that the ground-state of the neutral B_{38} final state upon electron detachment is probably not a closed-shell species.

3.2. The photoelectron spectrum of B_{37}^-

The spectrum of B_{37}^- was well resolved and nine spectral bands could be identified and labeled as X, A–H in Fig. 1c. The peak maximum of band X defines the ground-state VDE of 3.88 eV. The ADE or electron affinity of B_{37} was evaluated from the onset of band X to be 3.76 ± 0.05 eV. The VDEs for bands A–H could all be readily measured from their band maxima and are given in Table S1.†

4. Theoretical results

The global minimum structures of B_{38}^- (**1**, C_s, ^{2}A″) and B_{37}^- (**2**, C_1, ^{1}A) are shown in Fig. 2. Alternative low-lying isomers within 1.5 eV are given in Fig. S1 and S2,† for B_{38}^- and B_{37}^-, respectively. Their configurational energy spectra are given in Fig. 3 with selected structures indicated.

4.1. The global minimum and low-lying isomers of B_{38}^-

The cohesive energy trend for B_n (n = 7–40) presented in the previous study on the B_{40}^- borospherene suggested a 2D to 3D cage structural transition for neutral B_n clusters at $n \approx 38$.[22] A subsequent DFT calculation showed that the B_{38} cluster has a D_{2h} cage global minimum with a low-lying 2D isomer consisting of a DHV.[33] More accurate calculations found that the 2D structure was slightly lower in energy than the D_{2h} B_{38} cage structure.[34] The current global minimum searches, in conjunction with full structural optimizations at PBE0/6-311+G*, found the same 2D isomer **1** (C_s, ^{2}A″) as the overwhelming global minimum for B_{38}^-, as shown in Fig. 2 and 3a. The

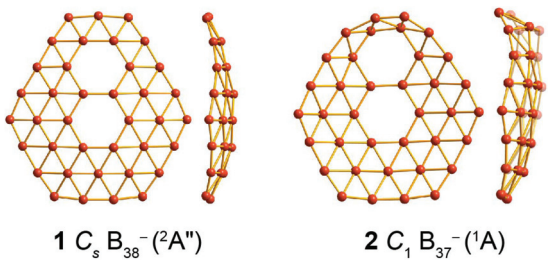

Fig. 2 The top and side views of the global minima of B_{38}^- and B_{37}^- at the PBE0/6-311+G* level.

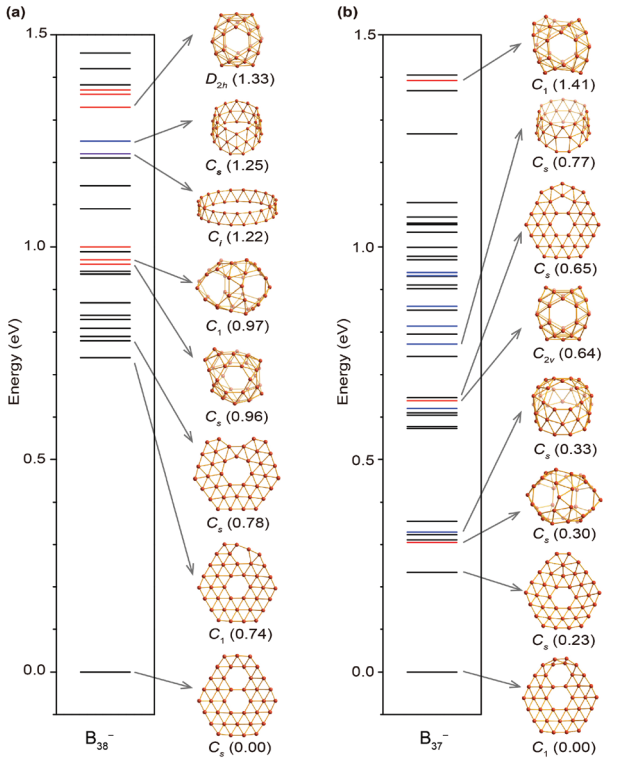

Fig. 3 The configurational energy spectra of (a) B_{38}^- and (b) B_{37}^- at the PBE0/6-311+G* level. Black, red, violet, and blue horizontal lines represent quasi-planar, cage-like, double-, and triple-ring tubular structures, respectively. Relative energies are given in eV.

second lowest-lying isomer, which is also 2D (C_1), lies 0.74 eV higher in energy.

The global minimum of B_{38}^- can be derived from the B_{35}^- cluster by simply adding three B atoms to its thinner edge (the top row in **1**), retaining the DHV first observed in the global minimum of B_{35}^-.[21] It is similar to the low-lying 2D isomer of neutral B_{38} (C_s, $^1A'$), which was found to be nearly degenerate with the D_{2h} cage isomer.[33] Surprisingly, the cage-like B_{38}^- (D_{2h}, $^2B_{2u}$) lies 1.33 eV higher than the 2D global minimum (Fig. 3a). In fact, the first nine isomers above the global minimum are all 2D with one or two polygonal vacancies (Fig. 3a and S1†), with the nearest isomer being at least 0.74 eV higher in energy. The stabilization of the 2D structure in the anion is a result of the delocalization of the additional electron, whereas the large HOMO–LUMO gap in the D_{2h} cage isomer means that the additional electron in the anion would occupy a much higher energy orbital, similar to the case of B_{40}^-.[22,23] Double- and triple-ring tubular-type isomers for B_{38}^- are at least 1.2 eV above the 2D global minimum.

4.2. The global minimum and low-lying isomers of B_{37}^-

The spectral pattern of B_{37}^- was somewhat similar to that of B_{38}^- (Fig. 1) and both have relatively high ADEs, suggesting that they might have similar structures. Hence, we built the initial structures of B_{37}^- by removing one B atom from the shorter edge of C_s B_{38}^- (**1**) or adding two B atoms to the thinner edge of B_{35}^-. Full structural optimization at PBE0 led to the 2D isomer of C_1 B_{37}^- (**2**, ^1A) as shown in Fig. 2. Because there were only two B atoms in the top row, significant local distortions were found upon optimization. The C_1 isomer was subsequently located as the global minimum for B_{37}^- (Fig. 3 and S2†) from minima-hopping searches.

As shown in Fig. 3b and S2,† the second lowest-lying isomer is also 2D (C_s, $^1A'$) at 0.23 eV above the global minimum. This isomer contains a hexagonal vacancy and can be viewed as adding a B atom to the edge of the hexagonal B_{36}^- cluster[20] with some major local rearrangement. The third isomer C_s B_{37}^- ($^1A'$) at 0.30 eV is cage-like, similar to the metallo-borospherene $Ca@B_{37}^-$.[49] The higher energy isomers of B_{37}^- display both 2D and 3D structures, which are generally similar to those of B_{38}^- (Fig. 3).

5. Comparison between experiment and theory

5.1. B_{38}^-

Since the global minimum 2D structure with a DHV for B_{38}^- (**1**, C_s, $^2A''$) is overwhelmingly favored from our global search, no higher energy isomers need to be considered in comparison with the experimental spectrum. The calculated VDEs of **1** at TD-PBE0 are compared with the experimental data in Table S1† and the simulated spectrum is compared with the experiment in Fig. 1b. The electronic structures of B_{38}^- and B_{38} are complicated, because of the open-shell nature of B_{38}, as hinted by the photoelectron spectrum (Fig. 1a).

The spin-polarized orbital energy order of **1** is shown in Fig. S3.† The unpaired CMO is the α-26a″ (shaded in pink), whereas the highest occupied α and β spins both belong to the 32a′ CMO, with little spin-polarization (within 0.001 eV). Consequently, upon detaching an electron from the highest α and β spins, we can reach both a triplet and a singlet final state, which are expected to be nearly degenerate competing for the ground electronic state of neutral B_{38}. At the PBE0 level, the first detachment channel is from β-32a′ with a calculated VDE of 4.125 eV for the triplet neutral final state ($^3A''$), whereas the detachment of α-32a′ gives a computed VDE of 4.126 eV for an open-shell singlet final state ($^1A''$). Both values are close to each other and are in good agreement with band X (experimental VDE: 4.02 eV). The calculated ADE between **1** (C_s, $^2A''$) and C_s B_{38} ($^3A''$) is 4.06 eV, consistent with the experimental ADE of 3.91 eV. Band A at ~4.3 eV corresponds to detachments from β-31a′ and α-26a″ which lead to a triplet ($^3A'$) and a singlet ($^1A''$) final state, respectively. The calculated VDEs (4.27 and 4.34 eV, respectively) are also close to each other and are in good agreement with band A. The calculated VDEs for higher binding energy detachment channels are also in good agreement with the experimental bands (B, C, D, and E), as can be seen in Fig. 1b and Table S1.† Overall, the agreement between the simulated spectral pattern and the experimental spectrum is quite gratifying, considering the open-shell nature of both B_{38}^- and its neutral.

5.2. B_{37}^-

Since B_{37}^- has a closed-shell configuration, electron detachment from each CMO produces a doublet final state, giving rise to much fewer detachment channels relative to the open-shell B_{38}^-. The simulated spectrum and the calculated VDEs from the B_{37}^- global minimum are compared with the experiment in Fig. 1d and Table S1,† respectively. The theoretical first VDE from the HOMO (56a) is 3.75 eV, which is in good agreement with band X (VDE: 3.88 eV). The calculated ADE (3.67 eV) is also in good agreement with the experimental value of 3.76 eV. There is an excellent correspondence between all the higher detachment channels and the observed PES bands (Fig. 1c and d). The level of agreement between the theory and experiment is remarkable, confirming the 2D structure with a DHV (**2**) as the global minimum of B_{37}^-.

6. Structures and chemical bonding

6.1. Quasi-planar boron clusters with a double-hexagonal vacancy

The global minimum of B_{38}^- (**1**) containing a DHV is directly related to the observed B_{35}^- (ref. 21) by adding a three-atom row on the top of B_{35}^- (Fig. 2), yielding the elongated and bowl-shaped 2D structure (length: 9.9 Å; width: 9.55 Å) with six apexes. The B_{38}^- cluster can also be described as consisting of three cyclic rings of B atoms: the inner B_6 ring, a middle B_{13} ring, and an external B_{19} ring. The peripheral B–B bond lengths in B_{38}^- range from 1.58 to 1.66 Å, whereas the interior B–B bond lengths range from 1.64 to 1.84 Å. The shortest peripheral B–B bonds are associated with the six apex atoms. The shorter peripheral B–B bonds relative to the interior B–B bonds cause the bowl-shape of B_{38}^- with an out-of-plane distortion of 1.45 Å (**1**, Fig. 2).

The global minimum of B_{37}^- (**2**) can be obtained by either adding two B atoms to the top of B_{35}^- or removing a B atom from the top row of B_{38}^- with a significant local distortion. Thus, B_{37}^- differs from B_{38}^- by one less peripheral B–B bond. The out-of-plane distortion of B_{37}^- is increased to 2.31 Å.

Starting from B_{35}^-, the DHV seems to become a prevalent structural feature in 2D boron clusters. Even though the B_{40} borospherene cage is overwhelmingly the global minimum in the neutral,[22] the global minimum of B_{40}^- is in fact a 2D structure, which can be viewed as adding two B atoms on the top of B_{38}^-. It is remarkable that for both B_{38}^- and B_{37}^- the global minima with the DHV are significantly favored without competing low-lying isomers. It should be pointed out that, for smaller boron clusters in the size range from B_{24}^- to B_{29}^-, competing low-lying isomers were observed in each case.[18,23] It seems that the hexagonal vacancy, in particular the DHV, plays a major role in stabilizing the 2D structures for larger boron clusters.

6.2. Chemical bonding in B_{38}^- and B_{37}^-: boron analogues of coronene

The chemical bonding in B_{38}^- and B_{37}^- has been analyzed using the AdNDP method (Fig. 4). For B_{38}^-, we used its closed-shell dianion B_{38}^{2-} with 116 valence electrons (58 electron pairs) for the purpose of bonding analyses. We found that bonding in B_{38}^{2-} is similar to that in B_{35}^-. The external B_{19} ring and the inner B_2 bridge between the two hexagonal holes are described by 20 2c–2e σ bonds (Fig. 4a). The bonding between the DHV and the surrounding boron atoms is *via* 10 3c–2e σ bonds, whereas the bonding between the external B_{19} ring and the middle B_{13} ring is *via* 16 4c–2e σ bonds.

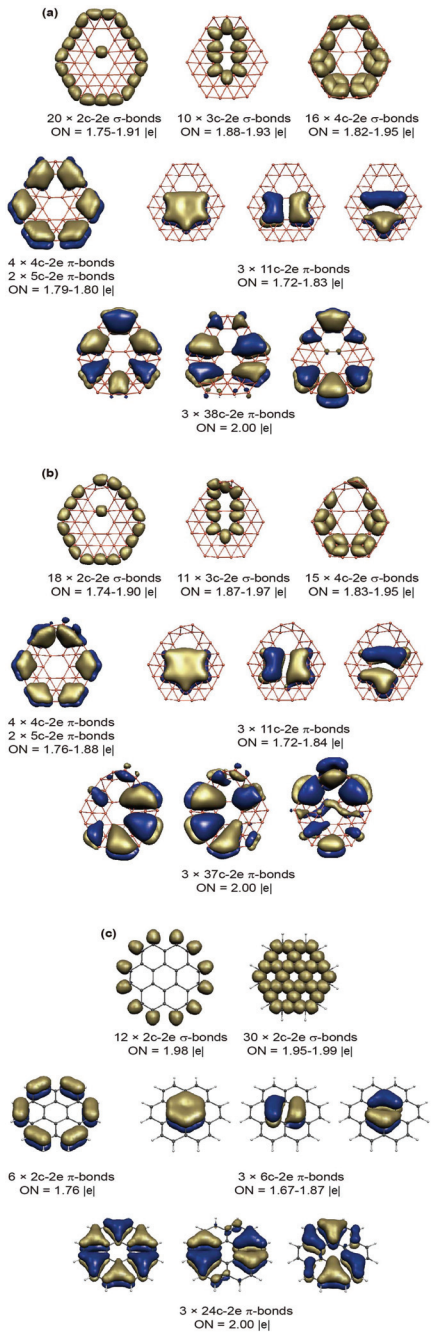

Fig. 4 Comparison of the AdNDP bonding patterns of (a) C_s B_{38}^{2-}, (b) C_1 B_{37}^-, and (c) coronene (D_{6h} $C_{24}H_{12}$). Occupation numbers (ONs) are indicated.

There are three types of π bonds in B_{38}^{2-}. We found six multi-center (four 4c–2e and two 5c–2e) π bonds around the six apex sites mainly involving bonding between the external B_{19} ring and the middle B_{13} ring. The inner B_6 ring involves in three 11c–2e π bonds, which are reminiscent of the π bonds in benzene. We also found three completely delocalized 38c–2e π bonds. The inner 11c–2e π sextet and the three 38c–2e π bonds form two aromatic systems conforming to the $(4n + 2)$ Huckel rule ($n = 1$), rendering dual π aromaticity to both C_s B_{38}^{2-} and the parent B_{38}^{-} (the missing electron in C_s B_{38}^{-} is from a σ orbital, Fig. S3†).

The bonding in B_{37}^{-} is very similar to that in B_{38}^{2-}. Except the fact that B_{37}^{-} has four fewer electrons than B_{38}^{2-} (all in the σ framework), the π bonding in the two systems is nearly identical according to the AdNDP analyses (Fig. 4b). Hence, B_{37}^{-} can also be considered to possess dual π aromaticity. More interestingly, we found that the π bonding patterns in both B_{37}^{-} and B_{38}^{2-} are very similar to that in the polycyclic aromatic coronene ($C_{24}H_{12}$) (Fig. 4c). Comparisons of their π CMOs are presented in Fig. S4† which provide further evidence to support this analogy. Thus, B_{37}^{-} and B_{38}^{-} can be considered as all-boron analogues of coronene $C_{24}H_{12}$, continuing the hydrocarbon analogy of all 2D boron clusters studied thus far.[11,17,23,24]

6.3. B_{38}^{-} and B_{37}^{-} as motifs for borophenes

Since the first successful characterization of graphene, there has been intense interest in finding new 2D materials. Even though boron does not have a layered allotrope, single-walled boron nanotubes were suggested, using boron sheets made of a triangular lattice.[50,51] The triangular lattice can be viewed by filling a boron atom to the hexagons of a graphene-like structure. However, such a triangular lattice is too electron-rich and undergoes distortion to a rippled boron layer.[52–55] DFT calculations suggested that a triangular lattice with periodic hexagonal vacancies would be planar and would be more stable than a close-packed triangular lattice, more suitable for the construction of boron nanotubes.[56,57] Further DFT studies predicted many different monolayer borons with different hole patterns[58,59] and suggested that they could be formed on inert substrates, such as silver.[29,30] The discovery of the C_{6v} B_{36} cluster with a hexagonal vacancy provided the first indirect experimental evidence of the viability of atomically-thin borons and inspired the proposal of "borophene" to designate the potentially new class of 2D materials.[20] Subsequently, the B_{35}^{-} cluster with a DHV was found to be an even more flexible motif for borophenes with different hole patterns and densities.[21] Recently, two groups have independently prepared borophenes on silver substrates.[27,28] Even though the atomic resolution was not achieved in the STM characterization, the most stable structure seemed to be the so-called χ3-borophene, in which two columns of adjacent hexagonal vacancies are connected by zigzag BDCs,[28,31] suggesting the importance of BDCs in stabilizing both 2D borophenes and 0D borospherenes.[22,32]

The DHV in B_{38}^{-} and B_{37}^{-} is reminiscent of the most stable χ3-borophene and can be viewed as its motifs. Fig. 5 illustrates the relationship between B_{38}^{-} and the χ3-borophene. One can fuse four adjacent B_{38}^{-} units to form a hexagonal vacancy between them by connecting two B_{38}^{-} units head-to-tail in the vertical direction, sharing a B_7 double-chain and a B_4 rhombus between the two neighboring B_{38}^{-} units in the horizontal direction. On the basis of this 2D pattern, one can further extend the molecular sheet to χ3-borophene by removing some hexacoordinate capping B atoms in the vertical direction to form the continuous zigzag BDCs, as shown by the rows of the adjacent hexagonal vacancies in the background. The present discussion is a simple model illustrating the connection of the 2D boron clusters with a DHV to borophenes. It is conceivable that with increasing size 2D boron clusters with more than two adjacent hexagonal vacancies may be possible. Hence, borophenes may be viewed as extended 2D cluster species. Such clusters have been considered computationally.[60,61] It would be interesting to test if such clusters would exist experimentally in larger boron clusters. The existence of such large 2D boron clusters may provide information about the feasibility of free-standing borophenes.

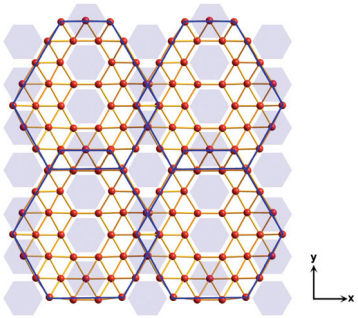

Fig. 5 Schematic of χ_3-borophene constructed by the 2D B_{38}^{-} motif (illustrated by blue solid lines). Shaded blue hexagons represent the hexagonal vacancies in χ_3-borophene.

7. Conclusions

The B_{38}^{-} and B_{37}^{-} clusters have been produced in the gas phase and characterized using anion photoelectron spectroscopy and theoretical calculations. The PE spectra were sufficiently well resolved and indicated that a single dominant isomer was the spectral carrier in each case. The most stable structures of B_{38}^{-} and B_{37}^{-} are established by comparisons of the experimental and computational data. Both clusters are found to adopt quasi-planar structures with a double-hexagonal vacancy, which seems to impart special stability to the large 2D boron clusters. Bonding analyses reveal that they are all-boron analogues of coronene, featuring unique dual π aromaticity. Such boron clusters with adjacent hexagonal vacancies may be used as structural motifs for χ3-borophenes, featuring rows of adjacent hexagonal vacancies connected by zigzag BDCs.

Acknowledgements

The experimental work was supported by the US National Science Foundation (CHE-1632813 to L. S. W.). We thank Dr Wei-Li Li and Dr C. Romanescu for experimental assistance. The theoretical work was supported by the National Natural Science Foundation of China (21373130 and 21573138), the National Key Basic Research Special Foundations (2011CB932401), and the State Key Laboratory of Quantum Optics and Quantum Optics Devices (KF201402).

Notes and references

1 B. Albert and H. Hillebrecht, *Angew. Chem., Int. Ed.*, 2009, **48**, 8640.
2 (*a*) R. Kawai and J. H. Weare, *J. Chem. Phys.*, 1991, **95**, 1151; (*b*) R. Kawai and J. H. Weare, *Chem. Phys. Lett.*, 1992, **191**, 311.
3 V. Bonacic-Koutecky, P. Fantucci and J. Koutecky, *Chem. Rev.*, 1991, **91**, 1035.
4 H. Kato, K. Yamashita and K. Morokuma, *Chem. Phys. Lett.*, 1992, **190**, 361.
5 (*a*) I. Boustani, *Int. J. Quantum Chem.*, 1994, **52**, 1081; (*b*) I. Boustani, *Phys. Rev. B: Condens. Matter*, 1997, **55**, 16426.
6 A. Ricca and C. W. Bauschlicher, *Chem. Phys.*, 1996, **208**, 233.
7 F. L. Gu, X. Yang, A. C. Tang, H. Jiao and P. v. R. Schleyer, *J. Comput. Chem.*, 1998, **19**, 203.
8 J. E. Fowler and J. M. Ugalde, *J. Phys. Chem. A*, 2000, **104**, 397.
9 H. J. Zhai, L. S. Wang, A. N. Alexandrova and A. I. Boldyrev, *J. Chem. Phys.*, 2002, **117**, 7917.
10 (*a*) H. J. Zhai, A. N. Alexandrova, K. A. Birch, A. I. Boldyrev and L. S. Wang, *Angew. Chem., Int. Ed.*, 2003, **42**, 6004; (*b*) L. L. Pan, J. Li and L. S. Wang, *J. Chem. Phys.*, 2008, **129**, 024302.
11 H. J. Zhai, B. Kiran, J. Li and L. S. Wang, *Nat. Mater.*, 2003, **2**, 827.
12 B. Kiran, S. Bulusu, H. J. Zhai, S. Yoo, X. C. Zeng and L. S. Wang, *Proc. Natl. Acad. Sci. U. S. A.*, 2005, **102**, 961.
13 A. N. Alexandrova, A. I. Boldyrev, H. J. Zhai and L. S. Wang, *Coord. Chem. Rev.*, 2006, **250**, 2811.
14 A. P. Sergeeva, D. Y. Zubarev, H. J. Zhai, A. I. Boldyrev and L. S. Wang, *J. Am. Chem. Soc.*, 2008, **130**, 7244.
15 (*a*) W. Huang, A. P. Sergeeva, H. J. Zhai, B. B. Averkiev, L. S. Wang and A. I. Boldyrev, *Nat. Chem.*, 2010, **2**, 202; (*b*) A. P. Sergeeva, B. B. Averkiev, H. J. Zhai, A. I. Boldyrev and L. S. Wang, *J. Chem. Phys.*, 2011, **134**, 224304.
16 (*a*) A. P. Sergeeva, Z. A. Piazza, C. Romanescu, W. L. Li, A. I. Boldyrev and L. S. Wang, *J. Am. Chem. Soc.*, 2012, **134**, 18065; (*b*) Z. A. Piazza, W. L. Li, C. Romanescu, A. P. Sergeeva, L. S. Wang and A. I. Boldyrev, *J. Chem. Phys.*, 2012, **136**, 104310.
17 A. P. Sergeeva, I. A. Popov, Z. A. Piazza, W. L. Li, C. Romanescu, L. S. Wang and A. I. Boldyrev, *Acc. Chem. Res.*, 2014, **47**, 1349.
18 (*a*) I. A. Popov, Z. A. Piazza, W. L. Li, L. S. Wang and A. I. Boldyrev, *J. Chem. Phys.*, 2013, **139**, 144307; (*b*) Z. A. Piazza, I. A. Popov, W. L. Li, R. Pal, X. C. Zeng, A. I. Boldyrev and L. S. Wang, *J. Chem. Phys.*, 2014, **141**, 034303; (*c*) X. M. Luo, T. Jian, L. J. Cheng, W. L. Li, Q. Chen, R. Li, H. J. Zhai, S. D. Li, A. I. Boldyrev and L. S. Wang, *Chem. Phys. Lett.*, 2016, DOI: 10.1016/j.cplett.2016.12.051; (*d*) W. L. Li, R. Pal, Z. A. Piazza, X. C. Zeng and L. S. Wang, *J. Chem. Phys.*, 2015, **142**, 204305; (*e*) Y. J. Wang, Y. F. Zhao, W. L. Li, T. Jian, Q. Chen, X. R. You, T. Ou, X. Y. Zhao, H. J. Zhai, S. D. Li, J. Li and L. S. Wang, *J. Chem. Phys.*, 2016, **144**, 064307; (*f*) H. R. Li, T. Jian, W. L. Li, C. Q. Miao, Y. J. Wang, Q. Chen, X. M. Luo, K. Wang, H. J. Zhai, S. D. Li and L. S. Wang, *Phys. Chem. Chem. Phys.*, 2016, **18**, 29147.
19 W. L. Li, Y. F. Zhao, H. S. Hu, J. Li and L. S. Wang, *Angew. Chem., Int. Ed.*, 2014, **53**, 5540.
20 Z. A. Piazza, H. S. Hu, W. L. Li, Y. F. Zhao, J. Li and L. S. Wang, *Nat. Commun.*, 2014, **5**, 3113.
21 W. L. Li, Q. Chen, W. J. Tian, H. Bai, Y. F. Zhao, H. S. Hu, J. Li, H. J. Zhai, S. D. Li and L. S. Wang, *J. Am. Chem. Soc.*, 2014, **136**, 12257.
22 H. J. Zhai, Y. F. Zhao, W. L. Li, Q. Chen, H. Bai, H. S. Hu, Z. A. Piazza, W. J. Tian, H. G. Lu, Y. B. Wu, Y. W. Mu, G. F. Wei, Z. P. Liu, J. Li, S. D. Li and L. S. Wang, *Nat. Chem.*, 2014, **6**, 727.
23 L. S. Wang, *Int. Rev. Phys. Chem.*, 2016, **35**, 69.
24 A. I. Boldyrev and L. S. Wang, *Phys. Chem. Chem. Phys.*, 2016, **18**, 11589.
25 E. Oger, N. R. M. Crawford, R. Kelting, P. Weis, M. M. Kappes and R. Ahlrichs, *Angew. Chem., Int. Ed.*, 2007, **46**, 8503.
26 C. Romanescu, D. J. Harding, A. Fielicke and L. S. Wang, *J. Chem. Phys.*, 2012, **137**, 014317.
27 A. J. Mannix, X. F. Zhou, B. Kiraly, J. D. Wood, D. Alducin, B. D. Myers, X. Liu, B. L. Fisher, U. Santiago, J. R. Guest, M. J. Yacaman, A. Ponce, A. R. Oganov, M. C. Hersam and N. P. Guisinger, *Science*, 2015, **350**, 1513.
28 B. Feng, J. Zhang, Q. Zhong, W. Li, S. Li, H. Li, P. Cheng, S. Meng, L. Chen and K. Wu, *Nat. Chem.*, 2016, **8**, 563.
29 (*a*) Y. Liu, E. S. Penev and B. I. Yakobson, *Angew. Chem., Int. Ed.*, 2013, **52**, 3156; (*b*) Z. Zhang, Y. Yang, G. Gao and B. I. Yakobson, *Angew. Chem., Int. Ed.*, 2015, **54**, 13022.
30 H. Liu, J. Gao and J. Zhao, *Sci. Rep.*, 2013, **3**, 3238.
31 (*a*) S. Xu, Y. Zhao, J. Liao, X. Yang and H. Xu, *Nano Res.*, 2016, **9**, 2616; (*b*) Z. Zhang, A. J. Mannix, Z. Hu, B. Kiraly, N. P. Guisinger, M. C. Hersam and B. I. Yakobson, *Nano Lett.*, 2016, **16**, 6622.
32 Q. Chen, W. L. Li, Y. F. Zhao, S. Y. Zhang, H. S. Hu, H. Bai, H. R. Li, W. J. Tian, H. G. Lu, H. J. Zhai, S. D. Li, J. Li and L. S. Wang, *ACS Nano*, 2015, **9**, 754.
33 J. Lv, Y. Wang, L. Zhu and Y. Ma, *Nanoscale*, 2014, **6**, 11692.
34 T. B. Tai and M. T. Nguyen, *Nanoscale*, 2015, **7**, 3316.

35 L. S. Wang, H. S. Cheng and J. Fan, *J. Chem. Phys.*, 1995, **102**, 9480.
36 (*a*) S. Goedecker, *J. Chem. Phys.*, 2004, **120**, 9911; (*b*) S. Goedecker, W. Hellmann and T. Lenosky, *Phys. Rev. Lett.*, 2005, **95**, 055501.
37 X. Chen, Y. F. Zhao, L. S. Wang and J. Li, *Comput. Theor. Chem*, 2007, DOI: 10.1016/j.comptc.2016.12.028.
38 L. Genovese, A. Neelov, S. Goedecker, T. Deutsch, S. A. Ghasemi, A. Willand, D. Caliste, O. Zilberberg, M. Rayson, A. Bergman and R. Schneider, *J. Chem. Phys.*, 2008, **129**, 014109.
39 S. Goedecker, M. Teter and J. Hutter, *Phys. Rev. B: Condens. Matter*, 1996, **54**, 1703.
40 J. P. Perdew, K. Burke and M. Ernzerhof, *Phys. Rev. Lett.*, 1996, **77**, 3865.
41 J. VandeVondele, M. Krack, F. Mohamed, M. Parrinello, T. Chassaing and J. Hutter, *Comput. Phys. Commun.*, 2005, **167**, 103.
42 J. VandeVondele and J. Hutter, *J. Chem. Phys.*, 2007, **127**, 114105.
43 C. Adamo and V. Barone, *J. Chem. Phys.*, 1999, **110**, 6158.
44 R. Krishnan, J. S. Binkley, R. Seeger and J. A. Pople, *J. Chem. Phys.*, 1980, **72**, 650.
45 R. Bauernschmitt and R. Ahlrichs, *Chem. Phys. Lett.*, 1996, **256**, 454.
46 M. J. Frisch, *et al.*, *Gaussian 09, Revision D.01*, Gaussian, Inc., Wallingford, CT, 2009.
47 D. Y. Zubarev and A. I. Boldyrev, *Phys. Chem. Chem. Phys.*, 2008, **10**, 5207.
48 U. Varetto, *Molekel 5.4.0.8*, Swiss National Supercomputing Center, Manno, Switzerland, 2009.
49 Q. Chen, H. R. Li, W. J. Tian, H. G. Lu, H. J. Zhai and S. D. Li, *Phys. Chem. Chem. Phys.*, 2016, **18**, 14186.
50 I. Boustani and A. Quandt, *Eurphys. Lett.*, 1997, **9**, 527.
51 A. Gindulyte, W. N. Lipscomb and N. L. Massa, *Inorg. Chem.*, 1998, **37**, 6544.
52 I. Boustani, A. Quandt, E. Hernandez and A. Rubio, *J. Chem. Phys.*, 1999, **110**, 3176.
53 M. H. Evans, J. D. Joannopoulos and S. T. Pantelides, *Phys. Rev. B: Condens. Matter*, 2005, **72**, 045434.
54 J. Kunstmann and A. Quandt, *Phys. Rev. B: Condens. Matter*, 2006, **74**, 035413.
55 K. C. Lau and R. Pandey, *J. Phys. Chem. C*, 2007, **111**, 2906.
56 H. Tang and S. Ismail-Beigi, *Phys. Rev. Lett.*, 2007, **99**, 115501.
57 X. Yang, Y. Ding and J. Ni, *Phys. Rev. B: Condens. Matter*, 2008, **77**, 041402(R).
58 E. S. Penev, S. Bhowmick, A. Sadrzadeh and B. I. Yakobson, *Nano Lett.*, 2012, **12**, 2441.
59 X. Wu, J. Dai, Y. Zhao, Z. Zhuo, J. Yang and X. C. Zeng, *ACS Nano*, 2012, **6**, 7443.
60 C. Ozdogan, S. Mukhopadhyay, W. Hayami, Z. B. Guvenc, R. Pandey and I. Boustani, *J. Phys. Chem. C*, 2010, **114**, 4362.
61 A. B. Rahane and V. Kumar, *Nanoscale*, 2015, **7**, 4055.